INTERNATIONAL SYMPOSIUM ON
DAMS FOR A CHANGING WORLD
-Need for Knowledge Transfer across the Generations & the World
Kyoto, Japan June 5, 2012

Theoretical Approach of Grouting Treatment for Fractured Rock

K. Kishida & T. Hosoda
Kyoto University, Kyoto, Japan
Kishida.kiyoshi.3r@kyoto-u.ac.jp

K. Kobayashi
Obayashi Co. Ltd., Tokyo, Japan

T. Fujita, H. Kishi & Y. Kuzuha
Japan Atomic Energy Agency, Tokai, Japan

J. Nobuto
Shimizu Co. Ltd., ToKyo, Japan

ABSTRACT:
Grouting technology is popular applied to dam foundation and tunnel excavation for the treatment of ground. Although there were several remarkable contributions for ground treatment, the mechanism and the theory, why the ground was treated effectively, are not clear yet. In this research work, the grout injection model of a single fracture, in which non-Newtonian fluid and the inertia term are considered, has been developed. Then, the grout injection experiments of a single fracture have been conducted and the numerical simulations have been also carried out. As compared our proposed model with well-known Gustafson and Stille model (GS model), the remarkable difference in grout penetration could not be clearly observed, except for the pressure at the aperture entrance and penetration velocity of the grout. Our proposed model could show the practical pressure behavior against GS model. Moreover, it can be also confirmed that the pressure at the fracture entrance had a temporary excess level against a set up level in the only initial time of simulations.

Keywords: Grouting, Rock Fracture, Non-Newtonian flow, Parallel plate injection test, Theoretical apporach

1. INTRODUCTION

Grouting is a technique which was developed to counteract the seepage from dam's reservoir, and its use has brought about a lot of important achievements in many fields such as dam foundations and tunnel excavations. On the other hand, the design and construction of grouting has always been done according to the results of experiments. This means that the injection technique and the quantitative evaluation used to make improvements are vague. The performance indices for the grout's waterproofing effect, on fractured rock masses in particular, should be the penetration length and/or the area along the fractures, considering the injection pressure and the grout material characteristics as the parameters. Grout material, in general, presents the yield behavior as Bingham flow. The influence of the grout injected into the fractures can be grasped, but the characteristics of the grout material itself as Bingham flow have not been sufficiently evaluated.

As for the injection technique into a single fracture, several research works had been conducted. Sato & Ito (1988), Nishigaki, et al. (2002 and 2003) and Wakita, et al. (2004) had carried out the routing injection experiments into a single fracture and had evaluated the injection area and the penetrated distance. In these research works, the yield phenomenon of the grouting material on the single fracture had been explained as the blockage and/or the clogging by particles of cement material. Therefore, the flow of the grouting had presented Newtonian flow. On the other hand, Hässler (1991) and Gustafson & Stille (1996) had discussed the grout flow as a Bingham flow. Gustafson & Stille (1996) had evaluated the maximum grout penetration of the parallel plate model in considering Bingham flow properties, such as yield stress and plastic viscosity.

In this study, the simulation model to estimate the flow of grout material considering Bingham fluid is developed. Using this model, experiments are simulated in which single fracture is injected with grout to examine such conditions as the time-dependency of the viscosity, the combination conversion, the pressure at the entrance to the fractures, the apertures of the fractures, and so on. In addition, the influence of sinusoidal model on the fracture wall is discussed as the simulation. Comparing the results of the experiments and the simulations, the

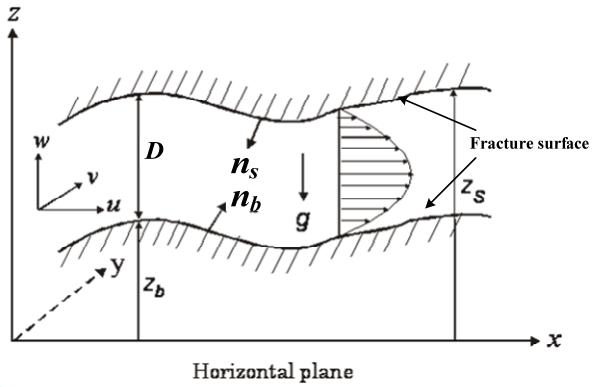

Figure 1. Conceptual flow model in a single fracture

validity of the proposed model and the flow behavior of the grout material are discussed.

2. GROUT PENETRATION MODEL OF PARALLEL PLATE SINGLE FRACTURE

Grout fluid is mainly treated as a non-Newtonian fluid because it solidifies after a certain period of time. In this study, the grout fluid is treated as a Bingham fluid which behaves as a rigid body at low levels of stress, but flows as a viscous fluid at the yield stress and higher.
Mgaya, et al. (2004) described Navier-Stokes equations at x-direction considering Fig. 1's conceptual fracture flow as follows:

$$\frac{\partial M}{\partial t}+\frac{\partial \beta M^2/D}{\partial x}+\frac{\partial \beta MN/D}{\partial y}=-\frac{\partial}{\partial x}\left(\frac{p_D}{\rho}D+\frac{gD^2}{2}\right)+\frac{p_D}{\rho}\frac{\partial z_s}{\partial x}-\left(\frac{p_D}{\rho}+gD\right)\frac{\partial z_b}{\partial x}-\frac{\tau_{sx}}{\rho}\sqrt{1+\left(\frac{\partial z_s}{\partial x}\right)^2+\left(\frac{\partial z_s}{\partial y}\right)^2}-\frac{\tau_{bx}}{\rho}\sqrt{1+\left(\frac{\partial z_b}{\partial x}\right)^2+\left(\frac{\partial z_b}{\partial y}\right)^2} \quad (1)$$

where, M and N are the flow flux in the x- and the y-directions, respectively. D is the aperture ($D = z_s - z_b$). z_s and z_b are the upper and the lower wall locations as shown in Fig. 1, respectively, from the datum plane. p_D is the pressure on the upper wall and g is the gravitational acceleration. τ_s and τ_b are the shear stress on the upper and the lower walls, respectively. ρ is the density of fluid and β is introduced here as a momentum correction factor.

Fig. 2 shows the grout injection model that we examine in this study. Grout fluid is injected into single fracture D from pressure device H at injection pressure P_g. We improve the point at which the injection speed reaches infinity at the beginning using Gustafson & Stille's model (1996). This is brought about by the discontinuity between groundwater pressure P_w on the fracture side and injection pressure P_g at the beginning (Fig. 2). Therefore, we consider an equation of motion for the

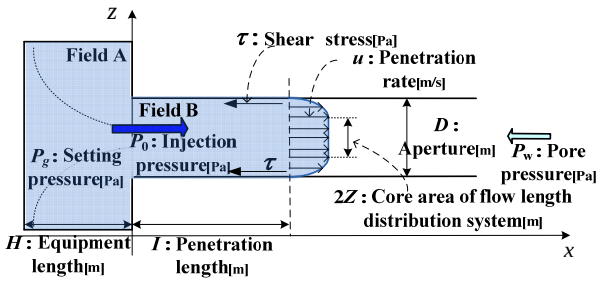

Figure 2. Grout injection model for the parallel plate

pipe axis in field A, which leads to Eq. 2, between the pressure at entrance P_0 and the injection pressure P_g, namely,

$$\left[\frac{d^2I}{dt^2}+\frac{1}{H}\left(\frac{dI}{dt}\right)^2\right]\cdot\frac{H}{2}=-\frac{P_0}{\rho}+\frac{P_g}{\rho} \quad (2)$$

At this time, pore water pressure P_w is ignored because it is much lower than the injection pressure. Bingham fluid has a field in which injection speed u remains constant in the area of the velocity distribution. We define this field as $2Z$, namely, the boundary of the grout fluid where the fracture is penetrated, as seen in Fig. 2. In addition, the wall shear stress acts when the grout fluid penetrates I, and it is possible to see the overshoot of the inside pressure. Based on these conditions, we obtain the following equation:

$$(H+2I)\cdot\frac{d^2I}{dt^2}+\left(\frac{dI}{dt}\right)^2+\frac{2\cdot\tau_Y}{\rho\cdot Z}\cdot I=\frac{2P_g}{\rho} \quad (3)$$

We define plastic viscosity μ and yield stress τ_Y. According to Hässler (1991), the velocity of grout dI/dt, moving in a horizontal fracture of aperture D, can be expressed as Eq. 4, namely,

$$v=\frac{dI}{dt}=\frac{\tau_Y D^2}{12\mu Z}\cdot\left\{1-3\frac{Z}{D}+4\left(\frac{Z}{D}\right)^3\right\} \quad (4)$$

Finally, solving Eqs 3 and 4, the grout penetration and elapsed time relation can be obtained in considering the effect of the inertia term.

3. GROUT INJECTION TEST ON PARALLEL PLATE MODEL AND ITS SIMULATION

3.1. Grout Injection Tests on Parallel Plate Model

In order to develop the low pH type grout material, the grout injection tests are conducted with a single fracture model by applying the parallel plate of aperture D and the influences of the grout material properties, the injection pressure and the aperture size are discussed In the experiment, injection pressure Pg is controlled by a

Table 1. Mechanical properties of grout material

Case	Plastic viscosity [mPa· s]	Yield stress [Pa]	Density [kg/m^3]	Injection Pressure [MPa]	Aperture by cubic law[mm]
Case 1	41.1	1.5	1230	0.15	0.206
Case 2	86.7	4.0	1250	0.48	0.104
Case 3	86.7	4.0	1250	0.14	0.197
Case 4	41.1	1.5	1230	0.15	0.094

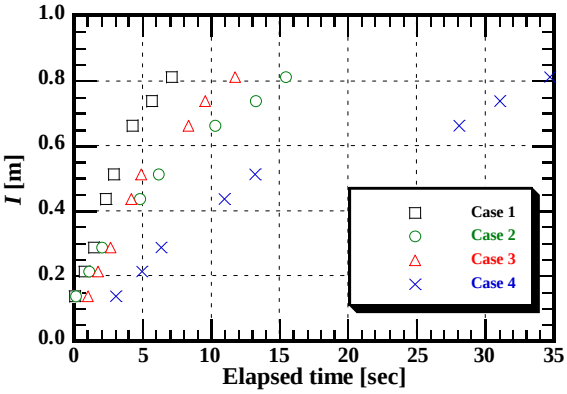

Figure 3. Penetration behavior of low pH cement type grout material through the parallel plate experiment.

pressure control device which is installed between field *A* and the entrance to the fracture. Therefore, from the beginning to the end of the test, the injection pressure is kept constant. The edge of the grout is measured by eyesight and we are able to take an actual measurement of the length of the grout. And, the weight of flow grout is measured at the end of parallel plate model. Table 1 shows the grout material properties and the experimental conditions.

Fig. 3 shows the grout penetration and elapsed time relation obtained through the grout injection tests. Compared Case 1 with Case 3, the grout material which presents high viscosity is observed the short of the penetration length. In the cases of the same material and the same injection pressure, on the other hand, it is confirmed that the penetration length externally decreases with the small aperture case. In cases of deferent aperture such as Case 2 and 3, the same penetration length can be observed with the arrangement of 3 times of the injection pressure. It is though the plastic viscosity of parallel plate injection test is deferent with that obtained through the element test such as the rheology measurement test. In the fracture, the shear resistance strongly affects to the grout penetration and the grout penetration length become shorter with the small aperture.

3.2. Comparison the Simulations with the Experiments

Fig. 4(a) shows the time variation for the penetration length using the GS model, the proposed model considering the inertia term, and the results of the experiment. In the experiment, it was impossible to measure more than about 0.8 m, the maximum range of the experimental equipment. As shown in Fig. 4, the penetration behavior of the two models was almost the same. On the other hand, comparing the two models with the experiment, the penetration length in the experiment is larger than in the other cases. On focusing at the initial phase of both simulations, the deference of the penetration distance can be observed in Fig. 4(b). Fig. 5 shows the time variation for the penetration rate and the injection pressure. This figure shows the comparison between the GS model and the proposed model. In the GS model, P_0 instantly becomes P_g and maintains a constant value. Starting at infinity, τ becomes smaller and smaller. However, this cannot explain why Bingham fluid has the property whereby it isn't able to flow unless the fluid increases to more than τ_Y. Taken together, the fluid starts to move instantly after the injection and becomes P_g.

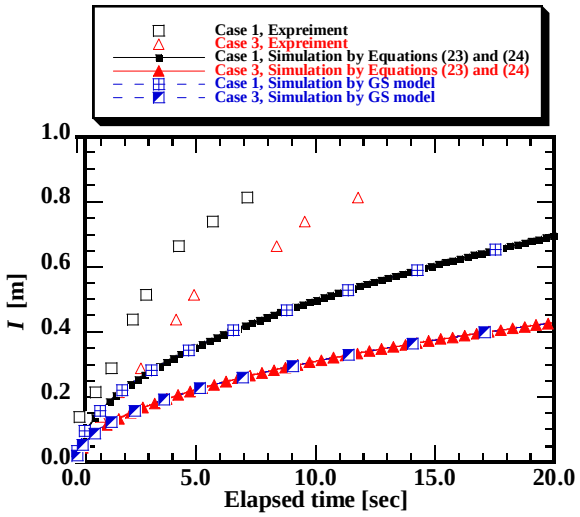

(a) Experiment vs. simulation

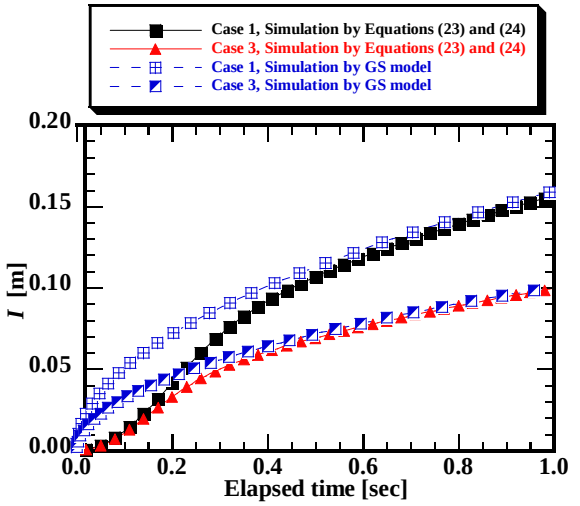

(b) Proposed model vs. GS model

Figure 4. The penetration distance are plotted through proposed model and GS model

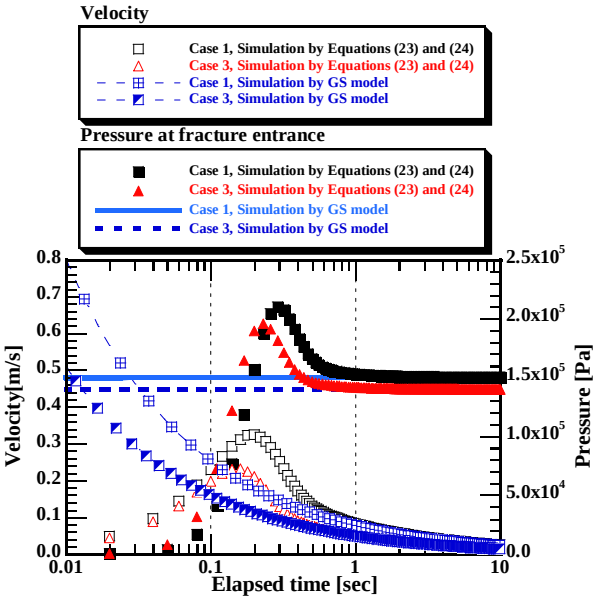

Figure 5. The penetration velocity – elapse time and the entrance pressure – elapse time relations are plotted through proposed model and GS model.

3.3. Influence of Fracture Roughness

In this research work, the fracture roughness simply assumes the sinusoidal model. Fig. 6 presents the grout injection model for sinusoidal single fracture. Here, we consider two cases. One is the case that the phases of the asperity are different π between upper and bottom fracture walls. The maximum grouting penetration is defined as follows:

$$l_1 = \frac{P_g \dfrac{D_o}{2\tau_Y}}{\left\{1+2\left(\dfrac{a}{D_o}\right)^2\right\}} = \frac{l_o}{\left\{1+2\left(\dfrac{a}{D_o}\right)^2\right\}} \qquad (5)$$

where, D_0 is the mean aperture and l_0 is the maximum grouting penetration at the parallel plate model (Aperture is D_0). On the other hand, the other one is the case that the phases of both fracture walls are the same. In this case, the phase lag is zero and the maximum grouting penetration is equal to the case of the parallel plate model as follows:

$$l_2 = P_g \frac{D_o}{2\tau_Y} = l_o \qquad (6)$$

In this research, the influence of sinusoidal fracture wall to the grout penetration is discussed with several cases as shown in Table 2. Basically, the first number of each case shows material type as shown in Table 1. The injection pressure of Case 1-1 to 2-3 is 0.136 MPa and Case 3-1 to 4-3 is 0.142 MPa.

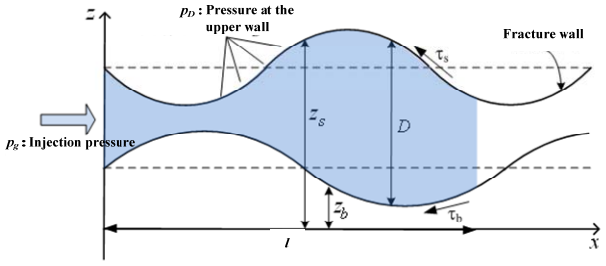

Figure 6. Grout injection model for sinusoidal single fracture

Table 2. Material parameters, mean aperture: D_0, maximum flow length at parallel plate model: l_0, amplitude: a, wave length: λ and phase: ϕ

Case	Material type	D_0 [mm]	l_0 [mm]	a [mm]	λ [mm]	ϕ
1-1	Case 2 or 3 in Table 1	0.197	3.35	0 ~ 0.05	1.0	π
1-2				0.05	$10 \sim 10^6$	π
1-3				0.05	1.0	0 ~ 2π
2-1		0.05	0.85	0 ~ 0.0125	0.25	π
2-2				0.0125	$10 \sim 10^6$	π
2-3				0.0125	0.25	0 ~ 2π
3-1	Case 1 or 4 in Table 1	0.206	9.75	0 ~ 0.05	1.0	π
3-2				0.05	$10 \sim 10^6$	π
3-3				0.05	1.0	0 ~ 2π
4-1		0.05	2.37	0 ~ 0.0125	0.25	π
4-2				0.0125	$10 \sim 10^6$	π
4-3				0.0125	0.25	0 ~ 2π

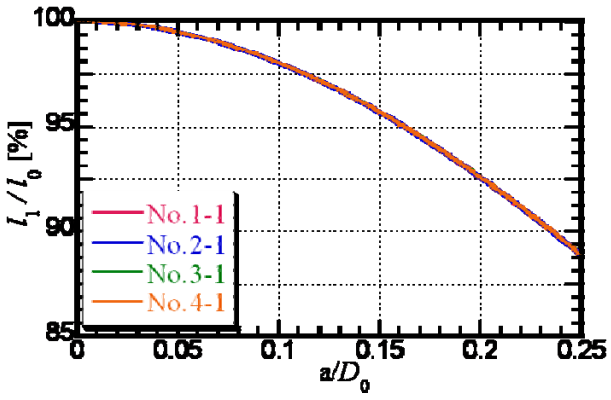

Figure 7. Amplitude variation in the maximum penetration distance through the simulations for the sinusoidal fracture model

Fig. 7 shows the maximum grout penetration and amplitude variation relation with the case of the fracture phase lag. In all cases, the maximum grout penetration decreases 88 % of the parallel plate model at 0.25 of a/D_0. The grout penetration strongly affects the amplitude of the fracture wall without the influence of material type, injection pressure and mean aperture. At 0.5 of a/D_0, the maximum grout penetration decreases 67 % of the parallel plate model.

Fig. 8 shows the maximum penetration distance and the

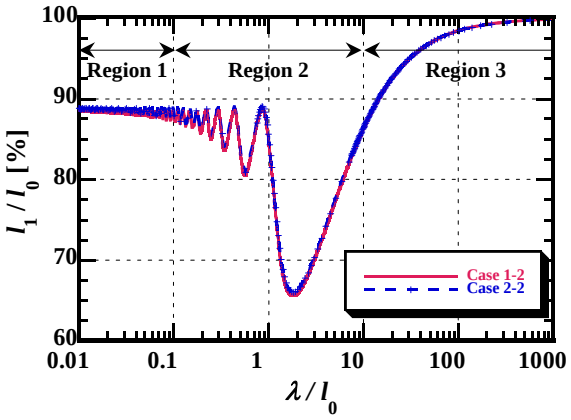

Figure 8. Wavelength variation in the maximum grout penetration through the simulations for the sinusoidal fracture

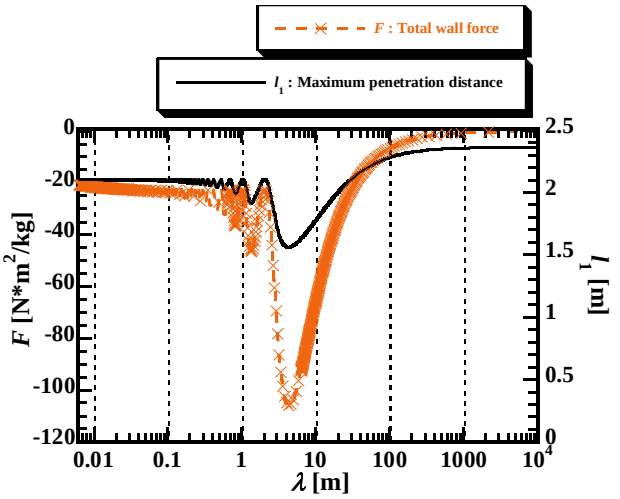

Figure 9. The Wall resistance force and wavelength of sinusoidal fracture wall relation and the maximum grout penetration and wavelength relation through the simulations for the sinusoidal fracture model.

wavelength relation in Case 1-2 and Case 2-2. In the region of relative short wavelength, the maximum grout penetration is 88 % of the parallel plate model. This is the same tendency of Fig. 7. When the wavelength becomes more 1/10 of the maximum grout penetration at the parallel plate model, the maximum grout penetration show the unstable tendency where indicates in Region 2 of Fig. 8. When the wavelength becomes larger than the maximum grout penetration of the parallel plate model, it is normal that the maximum penetration becomes that of the parallel plate model.

Fig. 9 shows the relationship between the accumulation of the wall resistance force and the wavelength and the relationship between the maximum grout penetration and the wavelength. The resistance force from the fracture wall of the flow direction is positive. It is confirmed that there is the closed relation between the accumulation of the resistance force and the maximum grout penetration. The accumulation of the resistance force of the wall becomes large at the location of the closed aperture and the maximum grout penetration becomes small. When the wavelength becomes larger than the maximum penetration of the parallel plate, the resistance force of the fracture wall becomes zero and the grout penetration becomes the maximum grout penetration of the parallel plate model.

4. CONCLUSIONS

In this study, a grout penetration equation considering the inertia term was presented and simulations were performed for the model experiment on grout injection. For the parallel plate model experiment on a single fracture, simulations were performed using the GS model and the model considering the inertia term. As a result, it was confirmed that for the time variation in the penetration length, it does not matter whether the inertia term is considered or not. On the other hand, it is possible to estimate the time variation in pressure, due to the changes in shape at the entrance, using the model which considers the inertia term.

In this study, in addition, the influences of both the asperities and the wavelength of sinusoidal fracture roughness were discussed for the maximum grout penetration length using our proposed simulation model. Consequently, it was confirmed that the maximum grout penetration decreased 88 % of the parallel plate model in considering the influence of asperities. As for the wavelength, moreover, 65 % reduction of the penetration against the parallel plate model was confirmed through the parametric simulation study. In the sinusoidal fracture model, it was thought that the flow resistance force on the fracture wall worked in the reverse direction of the grout flow.

ACKNOWLEDGEMENT

This work was conducted as a part of “The Project for Grouting Technology Development for Geological Disposal of HLW”, funded by the Ministry of Economy, Trade and Industry of Japan.

REFERENCES

Gustafson, G. and Stille, H. (1996): Prediction of groutability from grout properties and hydrogeological data”, Tunnelling and Underground Space Tech., 11(3), pp.325-332.

Hässler, L. (1991): Grouting of Rock –Simulation and Classification, Ph.D Thesis, Royal Institute of Technology.

Mgaya, P., Hosoda, T. and Kishida, K. (2004): Estimation of flow behavior on rock joints using the depth averaged flow model”, J. Applied Mechanics, JSCE, 7(II), pp. 1013 -1021.

Nishigaki, M., Komatsu, M., Yamamoto, H. and Mikake, S. (2002): Study on the properties of seepage flow and injection in the grouting for fractured rock masses, J. Geotechnical Engineering, JSCE, No. 715/III-60, pp. 311 -312. (in Japanese)

Nishigaki, M., Mikake, S., Komatsu, M. and KANKAM-YEBOAH, K. (2003): Study on the theoretical evaluation of grouting area and effective porosity for fractured rock masses”, J. Geotechnical Engineering, JSCE, No. 743/III-64,

pp. 199 – 212. (in Japanese)
Sato, K. and Ito, H. (1988): Clogging mechanism and time dependence of rock mass seepage, Soil mechanics and foundation engineering, JGS, 36(4), pp. 21-25. (in Japanese)
Wakita, S., Date, K., Yamamoto, T., Nakamura, Y., Mito, Y. and Aoki, K. (2004): Laboratory and field experiments on dynamic grouting and its analysis based on the grout penetration model, Proc. the 33rd Symp. of Rock Mech., JSCE, pp. 415-420. (in Japanese)